

Improvement in Oxidation Resistance of Stainless Steel by Molten-Salt Electrodeposition of La

Michihisa Fukumoto,*‡ Rie Yamashita,*† and Motoi Hara*

Received March 22, 2004; revised September 3, 2004

Improvement in the oxidation resistance of SUS304 stainless steel was accomplished by electrodeposition of La in a molten salt. The electrolysis of La was conducted using a potentiostatic-polarization method in an equimolar NaCl–KCl melt containing 3.5 mol.% LaF₃ at 1023 K. Observation of the specimen surface after polarization at -1.8 V (vs. Ag/Ag⁺ (0.1)) for 0.18 ks showed that La particles were uniformly dispersed on the surface. The oxidation resistance of the electrodeposited stainless steel was significantly improved as compared with the untreated stainless steel. The scale formed on the untreated stainless steel after oxidation was thick and consisted of Fe₂O₃ and Fe₃O₄, whereas the scale formed on the electrodeposited stainless steel was extremely thin, and mainly consisted of Cr₂O₃.

KEY WORDS: electrodeposition; cyclic oxidation; molten salt; stainless steel; lanthanum.

INTRODUCTION

It has been reported that the addition of a small quantity of a rare-earth element is effective^{1–4} for improving the cyclic oxidation of stainless steel. Based on this fact, several mechanisms have been suggested, one of which postulates that the small addition of a rare-earth element to the steel leads to “keying-on” of the protective scale consisting of Cr₂O₃ and Al₂O₃ due to the rare-earth oxide included in the scale.⁵ Rare-earth elements can be

*Department of Materials Science and Engineering, Faculty of Engineering and Resource Science, Akita University, Akita 010-8502, Japan.

†Present affiliation: Yazaki Corporation, Japan.

‡To whom correspondence should be sent. Tel.: +81-18-889-2426; fax: +81-18-837-0403; e-mail: fukumoto@ipc.akita-u.ac.jp

added as an alloying⁶ element or as an oxide.⁷⁻⁹ The addition of a rare-earth element to steel has the problem of raising the cost of the steel. Therefore, a method for the addition of the rare-earth element to only the surface, i.e. by ion implantation,¹⁰⁻¹² a coating (such as sol-gel coating¹³), sputter coating,¹⁴ and CVD coating,¹⁵ have also been investigated. These investigations showed that oxidation resistance is improved by the addition of a rare earth element to only the surface. In the present study, a rare-earth element was deposited on the stainless-steel surface by a new method, that is, molten-salt electrodeposition.

Although electroplating using an aqueous solution as the electrolyte has been widely used, the materials which can be electroplated from aqueous solutions are limited. It is difficult for metals having electroplating potentials lower than the reduction potential of water to be electroplated from an aqueous solution. Rare-earth elements are such metals. However, for materials which cannot be electroplated from an aqueous solution, electroplating may become possible using a molten salt as the electrolyte. We have focused on this point and succeeded in electroplating Si¹⁶, Ta¹⁷ and Al^{18,19} from a molten salt. Electroplating these elements led to an improvement in the corrosion-resistance of the substrate material.

In the present study, the electrodeposition of La on SUS304 stainless steel was performed by potentiostatic electrolysis using a molten salt. Furthermore, the isothermal and cyclic-oxidation resistances of the electrodeposited SUS304 stainless steel were evaluated and compared to that of the untreated SUS304 stainless steel.

EXPERIMENTAL PROCEDURES

SUS304 stainless steel was used for the cathode substrate. The chemical composition of the steel is shown in Table I. Coupons about 10 × 10 × 1 mm were cut from the steel sheet to obtain the cathode substrate. The sample surfaces were polished with #800 SiC paper and then ultrasonically washed in acetone. A covering material was not applied to the cathode sample. As a result, the entire surface of the sample was immersed in the molten salt. A graphite rod of 6 mm diameter and 50 mm length was used as the counter electrode. The salt used as the electrolyte was equimolar NaCl-KCl containing LaF₃.

Table I. Chemical Composition of SUS304 Stainless Steel (wt.%)

Fe	C	Si	Mn	P	S	Ni	Cr	Mo	Cu
Bal.	0.066	0.58	0.82	0.029	0.002	8.75	18.29	0.14	0.14

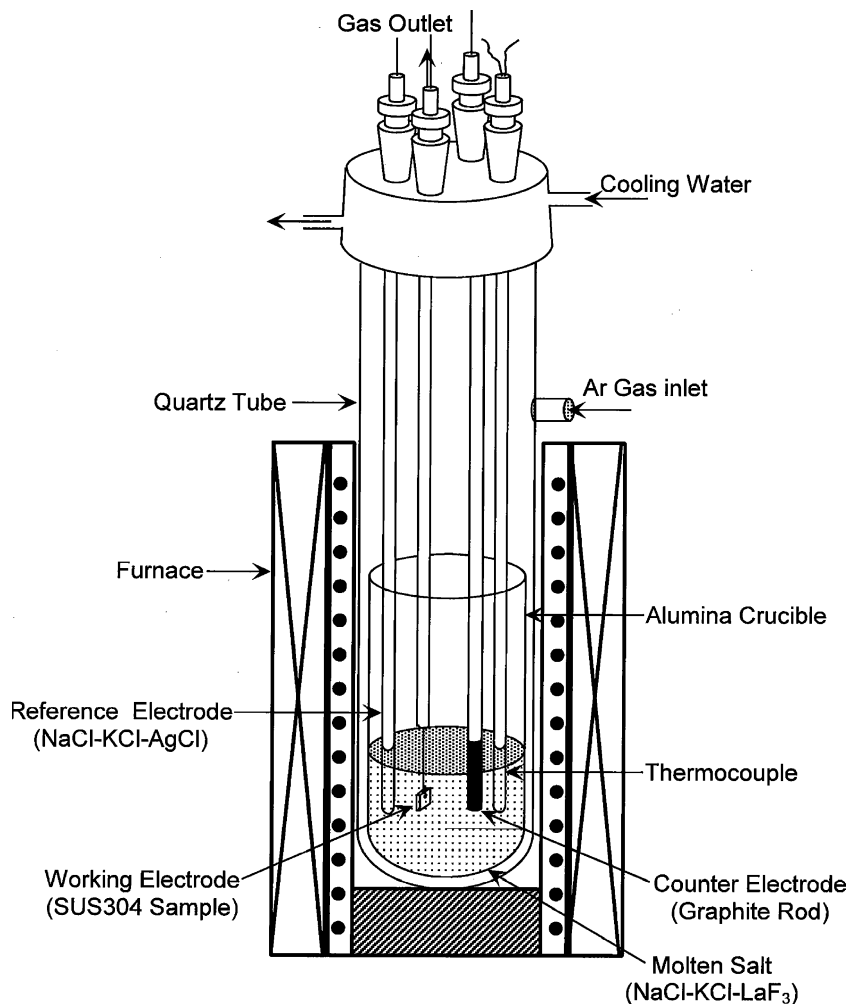


Fig. 1. Electrolytic cell for electrodeposition experiment.

Figure 1 is a schematic illustration of the electrolysis cell. During electrodeposition, Ar gas was introduced into the cell with a flow velocity of $3.3 \times 10^{-6} \text{ m}^3 \cdot \text{s}^{-1}$. The reference electrode was a Ag wire immersed in a NaCl-KCl-AgCl (45:45:10 mol.%) salt mixture, which was put into a mullite tube with a 6 mm outside diameter and 500 mm length. The potential values are given with reference to Ag/Ag⁺(0.1) at 1023 K.

In order to examine the cathodic-reduction behavior of the La³⁺ ion in a NaCl-KCl melt at 1023 K, the cathodic-polarization curve was

measured by the potential-sweep method at a sweep rate of $1.7 \times 10^{-3} \text{ V} \cdot \text{s}^{-1}$. The electrodeposition was carried out using potentiostatic polarization at the reduction potential of La^{3+} ion for 0.18 ks. During the potentiostatic polarization, the cathodic current was measured.

After electrodeposition, the specimen was taken out of the molten salt and its surface was water-washed to remove the adhering salt. The surface of the specimen was observed by a scanning-electron microscope (SEM) and analyzed by electron-probe microanalysis (EPMA). The deposited material was identified by X-ray diffraction with $\text{Cu K}\alpha$ radiation.

In order to evaluate the oxidation resistance of the sample after electrodeposition, isothermal-oxidation tests (thermogravimetry) of the SUS304 stainless steels with and without electrodeposition were carried out of 1073 and 1173 K in air. The cyclic-oxidation experiments were also carried out in air to examine the cyclic-oxidation behavior after electrodeposition. For the experiment, each cycle consisted of a heating for 36 ks at 1173 K and cooling for 0.3 ks.

RESULTS

Cathodic-Polarization Behavior

Figure 2 shows the cathodic-polarization curves of SUS304 stainless steel at 1023 K in a NaCl-KCl molten salt with and without 3.5 mol.% LaF_3 . For the molten salt without LaF_3 , a cathodic current was hardly observed in the NaCl-KCl molten salt even if the potential was decreased to -2.2 V , but a rise in the cathodic current due to the reduction of Na^+ or K^+ was observed in the potential range less noble than -2.2 V . For the molten salt containing LaF_3 , however, the cathodic current increased with a decrease in the polarization potential in the potential region below -1.5 V . In the potential region below -1.5 V , the cathodic current observed for the molten salt containing LaF_3 was greater than that for the molten salt without LaF_3 . Therefore, it is thought that for the molten salt containing LaF_3 , the cathodic-reduction reaction of the La^{3+} ion occurred in the potential region below -1.5 V .

Morphology and Composition of Electrodeposited Material

Figure 3 shows a scanning-electron micrograph of the surface of a sample after polarization at -1.8 V for 0.18 ks. For comparison, a micrograph of the surface of a sample before polarization is also shown. A deposit of particles whose diameter was below $1 \mu\text{m}$ was observed on the sample surface after polarization. These particles were uniformly distributed over the entire sample surface.

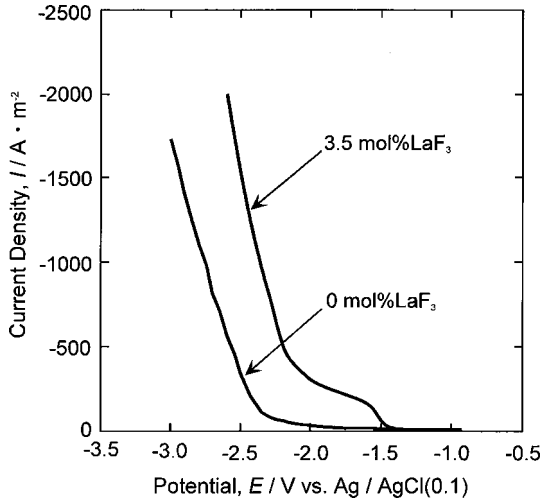


Fig. 2. Cathodic-polarization curves of SUS304 stainless steel measured at 1023 K in the NaCl–KCl melt with and without 3.5 mol.% LaF₃.

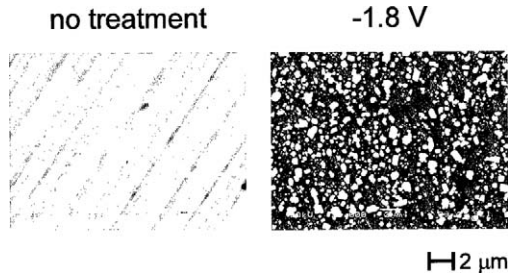


Fig. 3. Scanning-electron image of SUS304 stainless steel surface after potentiostatic polarization at -1.8 V for 0.18 ks in the NaCl–KCl melt containing 3.5 mol.% LaF₃. For comparison, the figure also includes a scanning-electron image of the surface of the untreated SUS304 stainless steel.

Figure 4 shows a scanning-electron micrograph with high magnification for the surface shown in Fig. 5 and the characteristic X-ray images of Fe, Cr, Ni and La for the surface. This showed that the white particles on the surface consisted of La. For the X-ray diffraction results, moreover, metallic La diffraction peaks were observed. Therefore, the white particles were identified as metallic La.

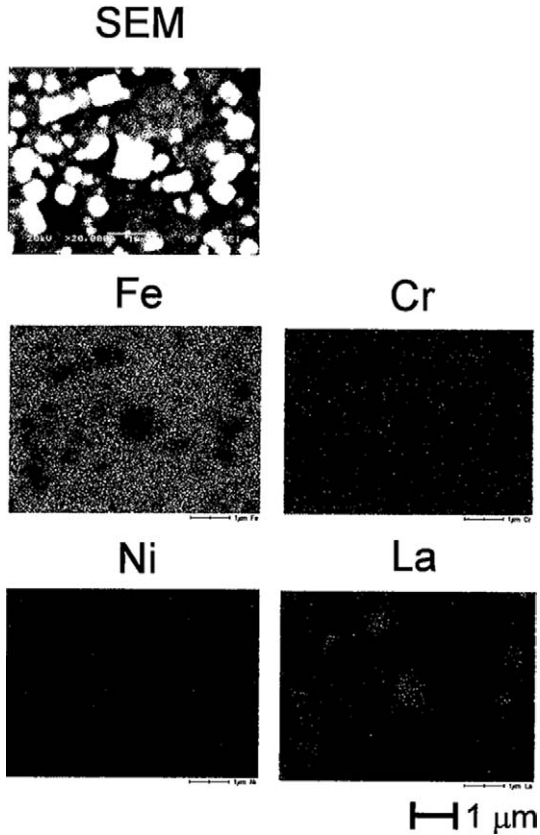


Fig. 4. Scanning-electron micrograph and characteristic X-ray images (Fe, Cr, Ni and La) of the surface of SUS304 stainless steel after potentiostatic polarization at -1.8 V for 0.18 ks in the NaCl–KCl melt containing 3.5 mol.% LaF_3 .

High-Temperature Oxidation Resistance of Specimens with Electrodeposited Material

Figure 5 shows the oxidation mass-gain curves at 1073 and 1173 K in air for SUS304 stainless steel electrodeposited at -1.8 V for 0.18 ks and untreated SUS304 stainless steel. It was found that the oxidation rates at both temperatures significantly decreased by performing the electrodeposition of La.

Figure 6 shows the cross-sectional micrographs (back-scattered-electron image; BEI) of the samples shown in Fig. 5. For the untreated steel, the scale

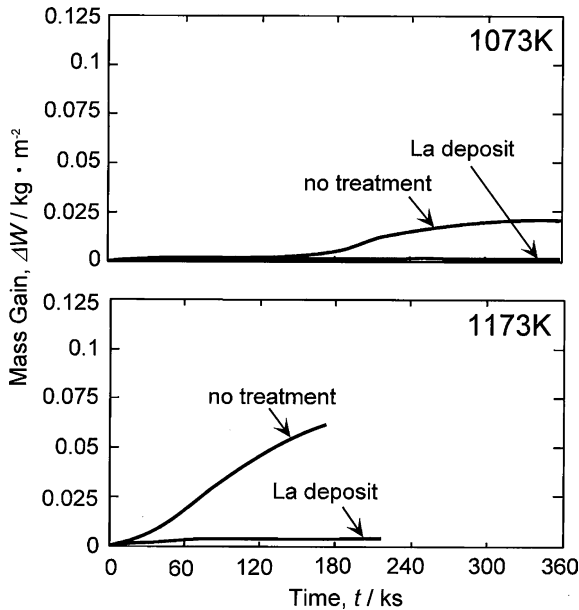


Fig. 5. Mass gain-time curves of SUS304 stainless steels with and without La deposit during oxidation at 1073 and 1173 K in air.

was thick. For the electrodeposited steel, the scale was extremely thin. For the untreated steel, the thickness of the scale formed at 1173 K was thinner than that at 1073 K because the outer layer of the scale formed at 1173 K spalled. It is found from X-ray diffraction and EPMA analysis that the scale formed on untreated steel consisted of Fe_2O_3 and Fe_3O_4 , while the scale formed on the electrodeposited steel consisted mainly of Cr_2O_3 .

Figure 7 shows the cycle-oxidation, mass-gain curves of electrodeposited and untreated SUS304 stainless steel at 1173 K in air. For the untreated steel, mass loss due to spalling of the scale was observed. On the contrary, for the electrodeposited steel, no mass loss was observed, while a slight mass gain was recognized.

Figure 8 shows the surface appearances of the samples after the oxidation shown in Fig. 7. The figure includes the surface appearances of the samples before oxidation. The spalling of much scale was observed for the untreated steel. For the electrodeposited steel, on the contrary, the scale was thin, and no spalling of the scale was observed.

Figure 9 shows some cross-sectional micrographs (back-scattered-electron image; BEI) and characteristic X-ray images of Fe, Cr, Ni and O of

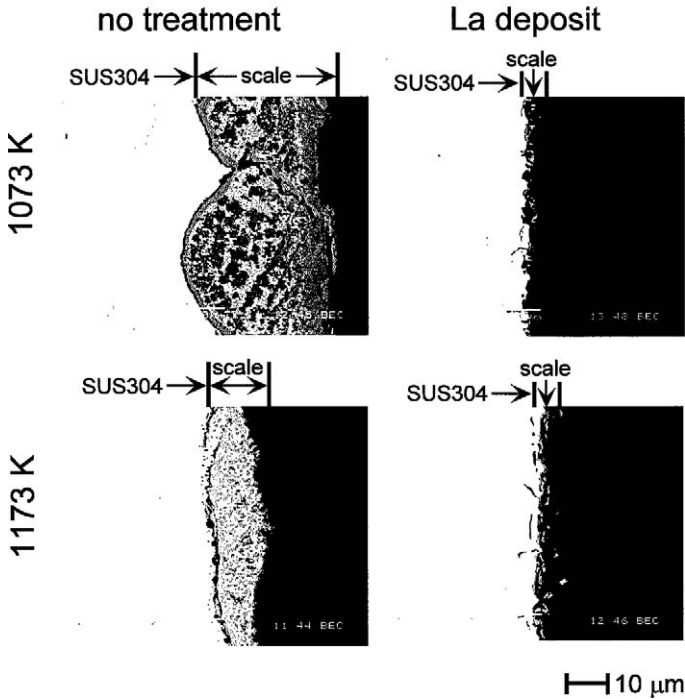


Fig. 6. S.E.M. Backscattered-electron images of the cross-sections of SUS304 stainless steels with and without a La deposit after isothermal oxidation at 1073 and 1173 K in air.

the samples shown in Fig. 10. For the untreated steel, the scale was thick. This sample underwent repetitive spallation of the scale due to the thermal cycling. Therefore, it is considered that the actual scale thickness was thicker than that of the observed scale. On the other hand, for the electrodeposited steel, the scale was thin. The thickness of this scale was less than $3\ \mu\text{m}$. For the electrodeposited steel, moreover, the formation of a wedge-shaped internal oxide is observed. The characteristic X-ray image of each element shows that the scale formed on the untreated steel contained Fe and Cr. On the other hand, for the electrodeposited steel, the scale consisted of Cr and did not contain other metallic elements. X-ray diffraction analysis showed that the scale formed on the untreated steel consisted mainly of Fe_2O_3 and Fe_3O_4 , while the scale formed the electrodeposited steel consisted mainly of Cr_2O_3 . It was found from EPMA analysis that the internal oxide observed for the electrodeposited steel was SiO_2 .

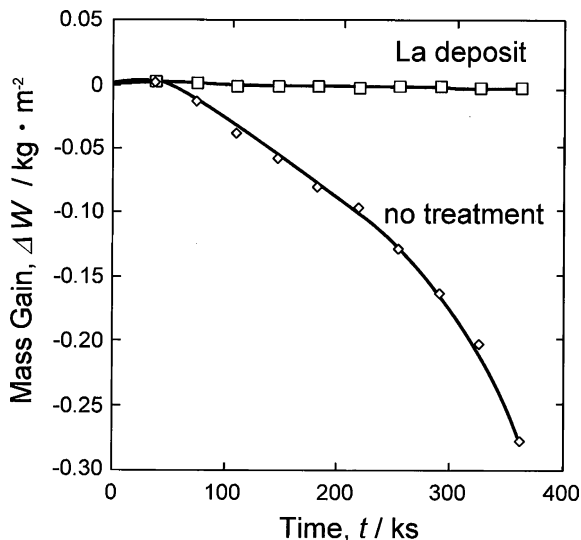


Fig. 7. Mass gain-time curves of SUS304 stainless steels with and without a La deposit during cyclic oxidation at 1173 K in air.

Figure 10 shows a scanning-electron micrograph of the surface of the electrodeposited samples before and after cyclic oxidation. It was found that the oxide particles, which look white in the scale formed after oxidation, were dispersed. EPMA analysis showed that these particles were an oxide containing La.

DISCUSSION

By using a molten salt as the electrolyte, the electrodeposition of La on SUS304 steel was performed, and the isothermal-oxidation resistance and the cyclic-oxidation resistance of the electrodeposited steel were investigated. As a result, for the electrodeposited steel, no rapid increase in mass gain was observed during isothermal oxidation, whereas the untreated steel showed a rapid increase in mass gain during isothermal oxidation. Moreover, during cyclic oxidation, no spallation of the scale was observed for the electrodeposited steel, while for the untreated steel, a mass loss due to spallation of the scale was observed. Therefore, it became clear that the oxidation resistance and the spallation resistance were improved by electrodeposition of La on the steel.

The effect of a rare-earth element on spallation of a scale has been investigated. Fujikawa *et al.*²⁰ added 0.03 wt.% Y to an austenitic stain-

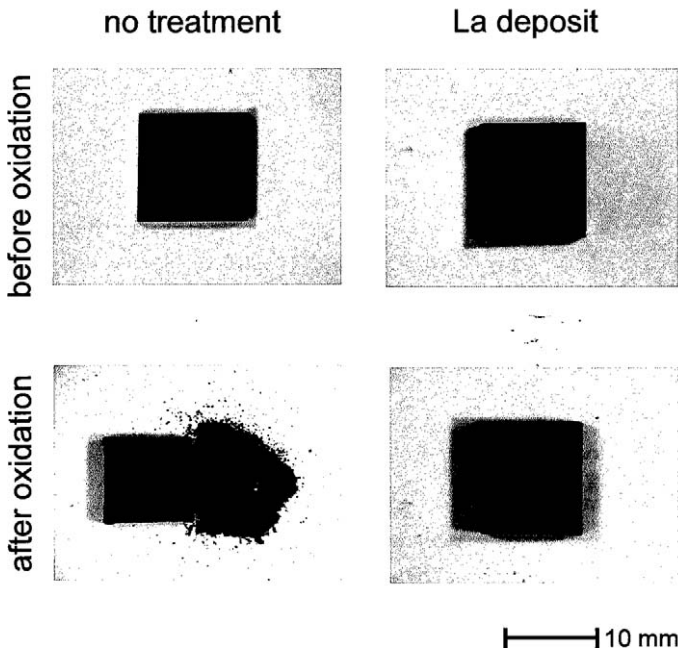


Fig. 8. Surface appearances of SUS304 stainless steels with and without a La deposit after cyclic oxidation for 360 ks at 1173 K in air.

less steel containing a small amount of Si. The oxidation resistance of this steel at 1173, 1273 and 1373 K in air, was studied and analyzed after oxidation using scanning-electron microscopy, secondary-ion mass spectroscopy, and transmission-electron microscopy. As a result, it was found that the segregation of Y at the oxide grain boundaries occurred, and inhibited the outward diffusion of cations, and promoted the internal oxide of Si. They presupposed that the formation of this internal oxide increased the spallation resistance of the scale. In the present study, as shown by cross-sectional observations, Figs. 6 and 9, a wedge-shaped internal oxide consisting of SiO_2 was observed for the electrodeposited steel. Therefore, it is thought that for the electrodeposited steel, the wedge-shaped internal oxide consisting of SiO_2 was formed according to the same mechanism that was proposed by Fujikawa *et al.*²⁰, and this oxide inhibited the spallation of the scale.

Bautista *et al.*²¹ added Y_2O_3 to sintered stainless steels (ferritic and austenitic steels), and examined the oxidation resistance of these steels. As a result, by adding Y_2O_3 , the oxidation resistance was improved, and the

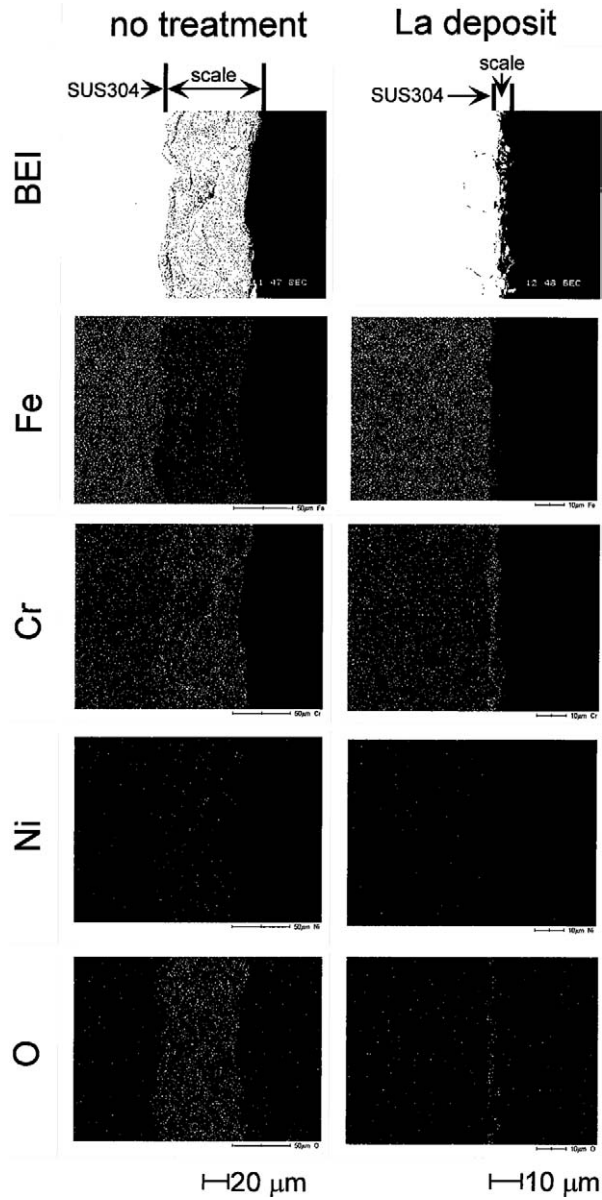


Fig. 9. Cross-sectional micrographs and X-ray characteristic images (Fe, Cr, Ni and O) of SUS304 stainless steels with and without a La deposit, after cyclic oxidation for 360 ks at 1173 K in air.

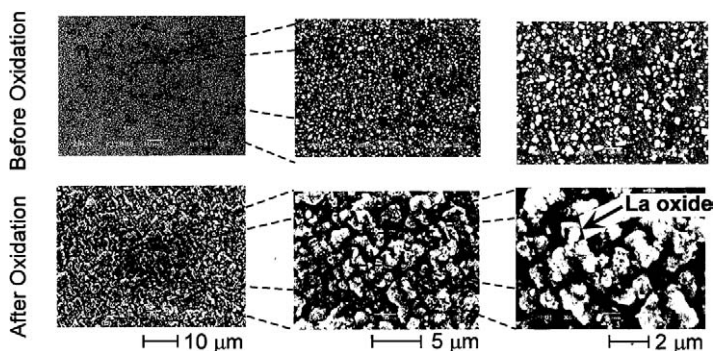


Fig. 10. Scanning-electron micrographs of SUS304 stainless steel surfaces after potentiostatic polarization at -1.8 V for 0.18 ks in the NaCl–KCl melt containing 3.5 mol.% LaF_3 at 1023 K, before and after cyclic oxidation for 360 ks at 1173 K.

spallation resistance was also remarkably improved during the cyclic oxidation. They explained the reason for this result as follows: for the growth of Cr_2O_3 , the inner diffusion of oxygen becomes dominant due to the formation of a rare-earth-element oxide. Therefore, the formation of voids at the scale/alloy interface was inhibited.¹³ As shown in the surface observation after oxidation in Fig. 10, La oxide particles were observed in the scale formed on the electrodeposited steel after oxidation. Therefore, it is postulated that spallation of the scale was inhibited by the effect of the rare-earth-element oxide contained in the scale as shown by Bautista *et al.*¹⁸

Riffard *et al.*²² coated Y by the sol–gel method on 304 stainless steel, and evaluated the oxidation resistance of this steel. As a result, they showed that for the Y-coated steel, a mass loss due to spallation of the scale rapidly increased, when the number of cycles increased during cyclic oxidation. In this study, although the coating of La was carried out on the stainless steel using electrodeposition, no mass loss was observed, even if the number of cycles increased. This observation seems to result from the following fact: since the electrodepositing was carried out at 1023 K, a part of the La dissolved in the matrix by mutual diffusion of the electrodeposited La and matrix. It is postulated that as the La dissolved in the matrix, high oxidation resistance was maintained, even if the number of cycles increased during the cyclic oxidation.

As mentioned above, this study suggests that the electrodeposition of a rare-earth element in a molten salt is a new process for the oxidation-resistant improvement of stainless steel.

CONCLUSIONS

La was electrodeposited on SUS304 stainless steel by potentiostatic-cathodic polarization in a NaCl–KCl molten salt containing LaF₃. The isothermal and cyclic oxidation resistances of the electrodeposited steel were evaluated. The following conclusions can be drawn.

1. The cathodic-polarization curve in the NaCl–KCl molten salt containing LaF₃ showed that the increase in the cathodic current is due to the cathodic reduction reaction of La³⁺.
2. On the surface of the electrodeposited steel, small particles consisting of metallic La were uniformly deposited.
3. The results of isothermal oxidation at 1073 and 1173 K showed that the oxidation resistance for the electrodeposited steel was much higher than that for the untreated steel.
4. The result of cyclic oxidation at 1173 K showed that a mass loss due to spalling of the scale was observed for the untreated sample, while for the electrodeposited sample no mass loss was observed. In this case, for the electrodeposited sample, the formation of a thin scale consisting mainly of Cr₂O₃ was observed.

REFERENCES

1. Y. Saito, K. Kiri, T. Kimura, T. Amano, and S. Yajima, *Journal of the Japan Institute of Metals* **39**, 1110 (1975).
2. Y. Saito, *Tetsu-to-Hagane* **65**, 747 (1979).
3. H. Hindam, and D. P. Whittle, *Oxidation of Metals* **18**, 245 (1982).
4. R. Cueff, H. Buscail, E. Caudron, C. Issartel, and F. Riffard, *Oxidation of Metals* **58**, 439 (2002).
5. K. Nishida, and T. Narita, collaboration Kinzokuno Kouonsanka Nyuumon, Maruzen (1988).
6. T. N. Rhys-Jones, H. J. Grabke, and H. Kudielka, *Corrosion Science* **27**, 49 (1987).
7. I. G. Wright, and B. A. Wilcox, *Oxidation of Metals* **8**, 283 (1974).
8. T. A. Ramanarayanan, R. Ayer, R. Petkovic-luton, and D. P. Leta, *Oxidation of Metals* **29**, 445 (1988).
9. B. A. Pint, and L. W. Hobbs, *Oxidation of Metals* **61**, 273 (2004).
10. V. A. C. Haanappel, Y. P. Jacob, and M. F. Stroosnijder, *Corrosion Science* **44**, 1411 (2002).
11. R. Cueff, H. Buscail, E. Caudron, C. Issartel, and F. Riffard, *Corrosion Science* **45**, 1815 (2003).
12. M. Li, Y. Qian, Y. Li, and Y. Zhou, *Oxidation of Metals* **61**, 529 (2004).
13. S. Roure, F. Czerwinski, and A. Petic, *Oxidation of Metals* **42**, 75 (1994).
14. D. A. Downham, and S. B. Shendye, *Oxidation of Metals* **43**, 411 (1995).
15. S. Chevalier, C. Nivot, and J. P. Larpin, *Oxidation of Metals* **61**, 195 (2004).
16. M. Hara, A. Honma, and Y. Sato, *Journal of Surface Finishing Society of Japan* **49**, 507 (1998).
17. M. Hara, Y. Sato, and T. Nakagawa, *Journal of the Japan Institute of Metals* **60**, 962 (1996).

18. M. Fukumoto, M. Hara, Y. Sato, T. Kidachi, and T. Nagataki, *Journal of the Japan Institute of Metals* **66**, 684 (2002).
19. M. Fukumoto, M. Hara, and T. Nagataki, *Zairyo-to-Kankyo* **51**, 510 (2002).
20. H. Fujikawa, T. Morimoto, Y. Nishiyama, and S. B. Newcomb, *Oxidation of Metals* **59**, 23 (2001).
21. A. Bautista, F. Velasco, and J. Abenojar, *Corrosion Science* **45**, 1343 (2003).
22. F. Riffard, H. Buscail, E. Caudron, R. Cueff, C. Issartel, and S. Perrier, *Corrosion Science* **45**, 2867 (2003).